A&A 417, L21–L24 (2004)
DOI: 10.1051/0004-6361:20040027

Astronomy & Astrophysics

VLT/NACO adaptive optics imaging of Titan⋆

E. Gendron[1], A. Coustenis[1], P. Drossart[1], M. Combes[1], M. Hirtzig[1], F. Lacombe[1], D. Rouan[1], C. Collin[1], S. Pau[1], A-M. Lagrange[2], D. Mouillet[2], P. Rabou[2], T. Fusco[3], and G. Zins[4]

[1] Observatoire de Paris, LESIA, UMR 8109 du CNRS, 5 place Jules Janssen, 92195 Meudon Cedex, France
[2] Laboratoire d'Astrophysique, Observatoire de Grenoble, BP 53, 38041 Grenoble, France
[3] ONERA – DOTA, 92322 Châtillon, France
[4] ESO, Karl-Schwarzschild -Str. 2, 85748 Garching bei München, Germany

Received 18 March 2003 / Accepted 17 January 2004

Abstract. The advent of the NAOS/CONICA adaptive optics system at the ESO Very Large Telescope recently gave us the opportunity to map the surface of Titan and to search for atmospheric variations at high spatial resolution and contrast. We report here the first results from a series of observations of Titan performed with this instrument in a number of near-infrared narrow-band filters, covering various altitude regions and three different longitudes (out of the 16 days of Titan's orbit). We have achieved unequaled contrast on images showing complex topography on Titan's trailing hemisphere and have found robust evidence for the north-south asymmetry inversion. The presence of other interesting atmospheric features at Titan's South Pole is described.

Key words. instrumentation: adaptive optics – planets and satellites: individual: Titan – infrared: solar system

1. Introduction

Despite its close exploration by the Voyager missions, many aspects of the atmosphere and surface of Titan remain currently unknown. Thus, the existence of seasonal or diurnal phenomena, the tropospheric content in condensates (clouds), the surface composition and topography are still under debate, although we have obtained many clues in the past decade, through spectroscopy and radar observations, but also by disk-resolved imaging. Besides the data obtained by the HST (Smith et al. 1996), Earth-based observations have been most valuable especially since the advent of the adaptive optics and related techniques which permit in the near-IR the sounding of the deeper atmosphere and surface of the satellite. For Titan the first results were obtained with the ESO ADONIS adaptive optics system in the mid-90s (Combes et al. 1997). Recently, a large set of new data was obtained from the CFHT, Keck and Gemini adaptive optics systems (Gibbard et al. 1999; Coustenis et al. 2001; Roe et al. 2002; Brown et al. 2002) and from the HST again (Meier et al. 2000) showing Titan's surface with the bright equatorial region (observed near 100 LCM on the leading side) and also darker areas in other parts of the disk. The trailing hemisphere has been under-observed until now and its more subtle structure obviously required higher-contrasted observations. Current surface models suggest all possible combinations between ices, liquid hydrocarbons, organics and rocks (e.g. Coustenis et al. 2001).

Send offprint requests to: E. Gendron,
e-mail: Eric.Gendron@obspm.fr

⋆ Based on observations collected at the European Southern Observatory, Chile (ESO Proposal 70.C-0588).

The situation in the lower atmosphere of Titan is also unclear. Evidence for tropospheric clouds has been found in spectra (Griffith et al. 2003) and references therein and in images of Titan (Roe et al. 2002; Brown et al. 2002), while other models and observations indicate that Titan's troposphere must be supersaturated in methane. Further up, in the stratosphere, adaptive optics images showed until recently the haze-sensitive north-south asymmetry with a brighter South Pole. This asymmetry was recently found to have reversed. Another bright atmospheric feature, noticed for the first time on Titan's morning limb, was interpreted as a diurnal effect (Coustenis et al. 2001).

Titan is the main target of the NASA/ESA Cassini/Huygens mission, which will investigate the satellite in situ. In the meantime, ground-based data are vital to optimize the return of the mission. Hence, the advent of the new adaptive optics system NACO in combination with the Very Large Telescope of ESO in Chile offers a unique opportunity to study the resolved Titan disk with high sensitivity and increased spatial resolution.

2. Data acquisition

Adaptive optics compensates for the image degradation due to atmospheric turbulence, thanks to active optical elements driven in real-time by a servo-loop.

2.1. The VLT adaptive optics system NACO

NACO (Rousset et al. 2002) is the state-of-the-art adaptive optics system of the ESO Very Large Telescope, the four european 8-m telescopes located at Mount Paranal, Chile. NACO equips the Nasmyth-B focus of the fourth telescope unit (Yepun).

NACO recently saw its first light on November 25th 2001 (Lagrange et al. 2002), and is now offered to the astronomical community.

NACO is the association of two instruments: the adaptive optics system NAOS, and the spectro-imager CONICA. The main technical features of NAOS are a piezo-stack deformable mirror with 185 actuators and a separate tip-tilt mirror, two selectable Shack-Hartmann wavefront sensors operating either in the optical (450−950 nm) or in the near-IR (800−2500 nm) range, both featuring up to 14×14 subapertures. NAOS has a field selector allowing to pick the reference source up to 55″ away, to track moving targets, to compensate for flexures (pointing model) and differential atmospheric dispersion. NAOS has 5 selectable dichroic beamsplitters, and delivers a corrected image to the spectro-imager CONICA in the spectral range 1−5 μm.

CONICA is equipped with a 1024×1024 pixel ALADDIN2 InSb detector, operated at 27 K, and sensitive in the 0.9−5 μm domain. The read-out noise is 40 e^- rms/pixel in double correlated sampling read-out mode, and can be as low as 10 e^- rms/pixel in Fowler sampling mode (mainly used in long integration times for spectroscopy). CONICA has 5 magnification optics, providing adequate Nyquist samplings across the 1−5 μm domain (0.01325″, 0.027″ and 0.054″). It is equipped with broadband, intermediate band ($R \approx 35$) and standard narrow-band filters (HeI, P_γ, FeII, H_2, Br_γ, all with $R \approx 90$). Due to the large telescope diameter, NACO gives access to small scales in imaging (e.g. 0.033″ at 1.28 μm).

Table 1. Titan[a] observational log.

Filter[b] (μm)	Lowest altitude region probed[c]	Number of images × int. time (s)
1.04	tropopause	4×20
1.08	surface + lower tropo	22×20
1.09	surface + lower tropo	20×20
1.24	upper troposphere	23×40
1.28	surface	21×40
1.64	low strato + tropo	7×200
1.75	stratosphere	7×200
2.12	troposphere	13×200
2.17	lowest strato + tropo	7×200

[a] The Titan observations were taken at SEP longitudes 76 to 79° for Nov. 20, 2002, 189.5 to 191° for the 25, and 211 to 214° for the 26. Star (or PSF) observations were acquired before and after the Titan observations in each filter.

[b] Central wavelength of the narrow-band filter (for details see `http://www.eso.org/instruments/naco/`).

[c] The filters can probe altitudes down to the region indicated. They range roughly as follows with increasing lowest altitude probed: 1.28 (P_β), 1.08 (HeI), 1.09 (P_γ), 2.12 (H_2 (1−0)), 1.24, 1.04, 2.17 (Br_γ), 1.64 (FeII), 1.75 μm.

2.2. Titan observations

Titan was the first extended planetary object to be observed scientifically by NACO. Images of Titan were obtained using 9 narrow-band filters which sampled wavelengths with large variations in methane opacity. This permitted sounding of different altitudes ranging from the stratosphere to the surface (see Table 1).

For each filter, the observations were performed by averaging several images (see Table 1) taken at random locations all over the array for a better averaging of the flat-field response. Integration times have been chosen so that individual images are photon noise limited on Titan's disk. The signal level was checked to be well inside the range of the linear response of the detector.

Titan was observed during NACO garanteed time on 2002 November 20th, 25th and 26th, between 6.00 UT and 9.00 UT, crossing the meridian around 6.30 UT. While Titan can be observed close to zenith at Mauna Kea (Saturn has a $\delta \approx 22°$), it culminates at Paranal at best at 46° from zenith, not optimal for adaptive optics.

The best seeing conditions were obtained on the night of the 26th, with a stable seeing of 0.9″ and a long correlation time ($\tau_0 \approx 15$ ms). This allowed us to attain the diffraction limit down to 1.24 μm (0.032″ resolution, as shown by the full width at half maximum of the point spread function of the calibration star). On the other nights the atmospheric conditions were rather poor and highly variable. The median seeing values were 1.1″ and 1.5″ respectively for the 20th and 25th (with peaks up to 2.8″), both nights with a fast phase evolution ($\tau_0 = 3$ ms). This led to the diffraction limit down to only 1.75 μm (0.05″ *FWHM*) on the 20th, and down to 2.17 μm (0.06″ *FWHM*) on the 25th.

During these 3 nights Titan was used as the reference source for the visible wave-front sensor, running at a frame rate of 240 Hz. The configuration of the wavefront sensor, and particularly the large pixel scale of 0.58″, was chosen to limit the increase of wave-front sensing noise due to the spatial extension of Titan. The loss in signal-to-noise on the wave-front sensor was equivalent to an increase of 0.5 mag. NACO performance is limited by noise for sources fainter than $m_R = 11$, and reaches its limiting magnitude around $m_R = 17$. Despite its spatial extension, for Titan the performance is limited only by the system speed and the mirror undermodeling error.

The same dichroic plate was kept to split light between wave-front sensing and imaging channels, for all the spectral filters used. All the images on CONICA are taken with the same pixel scale of 0.01325″/pixel.

Star observations were interweaved with the Titan observations in order to calibrate for the PSF used for deconvolution. Titan has a $m_V = 8.05$ and we chose the star HD 40329 as a reference ($m_V = 8.17$, SP = G5, located less than 3° away). The slight excess in star magnitude accounts for the increase of wavefront sensing noise due to the spatial extension (0.87″) of Titan.

3. Data processing

3.1. Image reduction

Accurate flat-fields were acquired on the twilight sky. Special care was devoted to the flat-field correction, as our previous experience showed that this effect may rapidly become a limiting factor when using deconvolution. By computing the ratio between flat-fields obtained from different data sets, we could estimate that our flat-field rms error is as low as 0.005. In addition, this number decreases as the square root of the number of averaged images taken at independent locations on the array (see Table 1).

The raw data were subtracted from the sky images, then divided by the flat-field response and corrected for dead pixels. Images were then recentered with sub-pixel accuracy using a cross-correlation method in a window of 3.4″ wide (256 pixels). Finally, a visual selection was used for eliminating the few bad quality images – if any.

Taking into account the camera read-out noise, the photon noise, and the flat-field compensation, we estimate the signal-to-noise ratio of the reduced images to range from 80 to 350 per pixel, depending on the wavelength.

3.2. Deconvolution and limb effects

The high signal-to-noise ratio of the images and the PSF calibrations allowed us to use and compare efficiently various deconvolution methods. We have tried several de convolution methods but present here the results from the Magain (Magain et al. 1998) and Bratsolis (Bratsolis & Sigelle 2001) codes, that were found efficient in the case of Titan. Thus, Fig. 2 shows images from our best observing night, all enhanced by use of the Magain method. The Bratsolis method is used for Fig. 3.

Following deconvolution, we modeled the center-to-limb effects to balance the contrast in the surface images (1.08 and 1.28 μm). The model takes into account fractal-shaped aerosols (Rannou et al. 1999) and various wavelength-dependent methane absorption coefficients and opacity. This correction was not applied to the atmospheric images so as not to hazard limb studies.

4. Results

Our new multi-wavelength Titan observations provided information at different atmospheric levels and on the surface (Table 1). A strong phase effect of 2.5° observed on the Western limb (left) of all of our images (Fig. 2), prohibited the detection of any morning features.

4.1. The atmospheric features

In our images taken at wavelengths containing atmospheric contribution, we find indication of the north-south asymmetry on Titan harboring its usual aspect (the southern "smile") at 2.12 μm, while the reversed situation is observed with filters probing higher altitudes, such as 1.64, 1.75 and 2.17 μm. An intermediate situation is observed for wavelengths near 1 μm, with both the bright southern and northern components present.

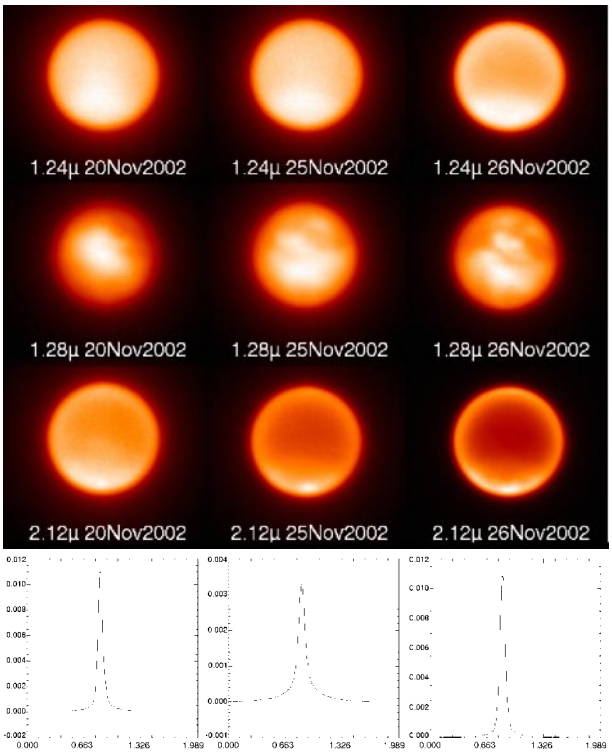

Fig. 1. Reduced images from the 3 nights, with variable seeing: it ranged from 0.8 (26th) to 2.8″ (20th). In all Titan images North is up and East-map is to the right. The PSF shown here correspond to the 1.28 μm filter.

A highly-contrasted (150% with respect to the limb) bright feature is observed at the South Pole and shown in our images taken at 1.24 and 2.12 μm on all dates; it is even clearly visible on our raw images (Fig. 1). This feature is not observed at the close-by 2.17-micron image, thus allowing us to discriminate in altitude and infer that the causing phenomenon is located somewhere in the atmosphere, at altitudes lower than 100 km. This feature is observed to vary in location on our images from one side of the south polar axis to the other within the week of our observations (Fig. 3). Thus, it lies at its furthest east on the 25th, while at its furthest west on the 20th. On the 26th, it seems to be centered upon the South Pole. We think of it as one large bright feature possibly related to a vortex near the Southern pole, for which further investigation is required. Other similar but less bright spots are seen on the south limb in particular in our 1.24 and 2.12 μm images on each side of this main feature.

4.2. The surface of Titan

During the night of November 20, at GEE, Titan's leading hemisphere shows the well-known bright feature at 1.08, 1.09 and 1.28 μm. The feature extends from +5° lat and 110° long to −45° lat and 50° long, and has a triangular drop-like shape with the narrower edge towards the south-east (Figs. 1 and 3). For the two other nights (November 25 and 26), closer to GWE, our NACO images show 4 bright areas: a double-peaked equatorial one with contrasts of 60−90% with respect to the

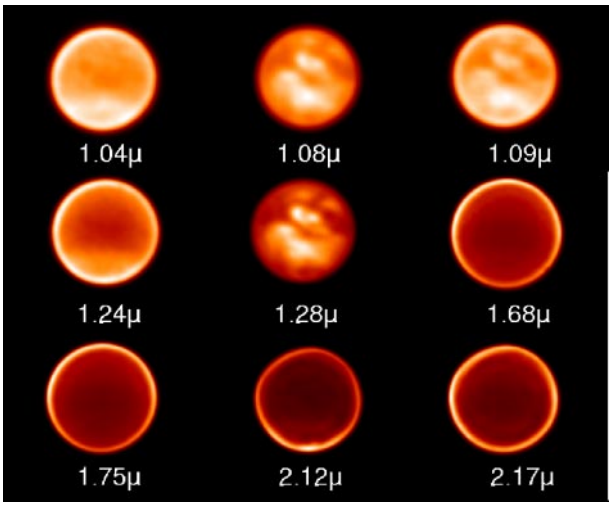

Fig. 2. Deconvolved images of Titan (using the Magain method) with limb correction for surface images (i.e. 1.08 and 1.28 μm) taken on November 26, 2002. The seeing is ~0.9″.

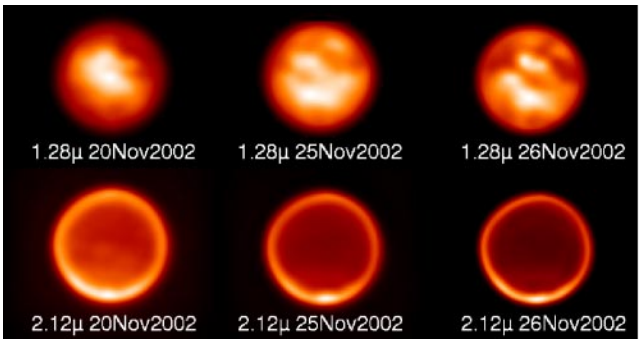

Fig. 3. Deconvolved (Bratsolis method) images of Titan and the evolution of its aspect as a function of time. The rotation of Titan's surface features is visible on the 1.28 μm images. The atmosphere (observed in the images at 2.12 μm) shows a bright southern limb, the phase effect on the western limb (to the left) and a highly-contrasted bright feature moving with time at the South Pole.

darkest zones in the image; another double-peaked one extending over 30° longitude in the south, with a contrast of about 80%; and finally two weaker northern areas of 40% contrast. These structures were hinted at in Keck speckle and adaptive optics images (Gibbard et al. 1999; Roe et al. 2002; Brown et al. 2002), but were observed by NACO at high contrasts.

For a comprehensive review on the possible surface components see Coustenis et al. (1995), Coustenis et al. (2001), Roe et al. (2002) and references therein.

5. Discussion and perspectives

Independent mapping of atmospheric phenomena and surface at a high spatial accuracy, achieved with NACO, successfully complements other large telescope observations of Titan in imaging, and HST. We have yet to model and interpret the physical and geophysical phenomena observed and to produce a full cartography of the surface.

We have not yet explored all the capabilities of NACO in the study of Titan. In particular, we plan to image Titan for the first time within the *L* and *M* bands in order to gain access to the 3 and 5 μm methane windows. We also plan to achieve long-slit imaging from 1 to 2.4 μm with $R \approx 1500$ and use the polarimetric mode.

The observations of NACO prepare the Cassini/VIMS (Visual and Infrared Mapping Spectrometer) observations (Brown et al. 2004), by determining the expected contrasts on surface and cloud features.

Acknowledgements. We thank P. Rannou for providing modeling of the center-to-limb effects. We are grateful to Emmanuel Bratsolis for use of his deconvolution algorithm.

References

Bratsolis, E., & Sigelle, M. 2001, A&A, 375, 1120
Brown, M. E., Bouchez, A. H., & Griffith, C. A. 2002, Nature, 420, 795
Brown, R. H., Baines, K. H., Belluci, G., et al. 2004, Space Sci. Rev., Cassini Issue (ed. C. T. Russell), accepted
Combes, M., Vapillon, L., Gendron, E., et al. 1997, Icarus, 129, 482
Coustenis, A., Lellouch, E., Maillard, J. P., & McKay, C. P. 1995, Icarus, 118, 87
Coustenis, A., Gendron, E., Lai, O., et al. 2001, Icarus, 154, 501
Gibbard, S. E., Macintosh, B., Gavel, E., et al. 1999, Icarus, 139, 189
Griffith, C. A., Owen, T. C., Geballe, T. R., et al. 2003, Science, 300, 628
Lagrange, A. M., Brandner, W., Chauvin, G., et al. 2002, Proc. SPIE, 4841
Magain, P., Courbin, F., & Sohy, S. 1998, ApJ, 494, 472
Meier, R., Smith, B. A., & Owen, T. C. 2000, Icarus, 145, 462
Rannou, P., McKay, C. P., Botet, R., & Cabane, M. 1999, Planet. Space Sci., 47, 385
Roe, H. G., de Pater, I., Macintosh, B. A., & McKay, C. P. 2002, ApJ, 581, 1399
Rousset, G., Lacombe, F., Puget, P., et al. 2002, Proc. SPIE, 4839, 140
Smith, P. H., Lemmon, M. T., Lorenz, R. D., et al. 1996, Icarus, 119, 336